Associated production of top squarks and charginos at the CERN LHC in NLO SUSY-QCD

Li Gang Jin, Chong Sheng Li*, and Jian Jun Liu

Department of Physics, Peking University, Beijing 100871, P.R. China

arXiv:hep-ph/0307390 v1 31 Jul 2003

Abstract

We calculate the next-to-leading order inclusive total cross sections for the associated production processes $pp \to \tilde{t}_i \tilde{\chi}_k^- + X$ in the Minimal Supersymmetric Standard Model at the CERN LHC. Our results provide the theoretical predictions for the total cross sections for the above processes. The NLO QCD corrections in general enhance the leading order total cross sections significantly, and vastly reduce the dependence of the total cross sections on the renormalization/factorization scale, which leads to increased confidence in predictions based on these results.

[Keywords: Top squark, Chargino, Supersymmetric QCD]

PACS numbers: 12.60.Jv, 12.38.Bx, 13.85.Fb

* E-mail: csli@pku.edu.cn

The CERN Large Hadron Collider (LHC), with $\sqrt{S} = 14$ TeV and a luminosity of 100 fb^{-1} per year [1], will be a wonderful machine for discovering new physics. In so many new physical models, the Minimal Supersymmetric Standard Model (MSSM) [2] is one of the most attractive models for the theorists and the high energy experimenters, and searching for supersymmetric (SUSY) particles, as a direct experimental evidence, is one of the prime objectives at the LHC. Therefore, a good understanding of theoretical predictions of the cross sections for the production of the SUSY particles is important. The cross sections for the production of squarks and gluinos were calculated at the Born level already many years ago [3]. To date, the productions of gluinos and squarks [4, 5], top squarks [6], sleptons [7, 8] and gauginos [7] at the hadron colliders in the next-to-leading order (NLO) also have been studied. And recently, the NLO SUSY-QCD analysis of the associated production of a gaugino ($\tilde{\chi}$) with a gluino ($\tilde{g}$) at the Tevatron and the LHC has been presented in Ref. [9].

In this Letter we report the NLO QCD (including SUSY QCD) calculation of the associated production of top squarks (stops) and charginos at the LHC. Similar to $pp \to gb \to tH^-$ [10], which is expected to be a dominate process for the charged Higgs boson production at the LHC, the associated production $pp \to gb \to \tilde{t}_i \tilde{\chi}_k^-$ may be also the dominate process for single top squark or chargino production at the LHC. This is due to the following reasons: first, the large top quark mass in stop mass matrix can lead to strong mixing, and induce large mass difference between the lighter mass eigenstate and the heavier one, which means that the phase space for the lighter stop will be great and benefit its production; second, besides containing a strong QCD coupling between the incoming partons, this process also includes an enhanced effect from the Yukawa coupling in the vertex $b - \tilde{t}_i - \tilde{\chi}_k^-$ of the final states. For simplicity, in our calculation, we neglect the bottom quark mass except in the Yukawa coupling. Such approximations are valid in all diagrams, in which the bottom quark appears as an initial state parton, according to the simplified Aivazis-Collins-Olness-Tung (ACOT) scheme [11]. However, it was pointed out in Ref. [12] that the approximations of the hard process kinematics and the introduction of conventional bottom quark densities will give rise to sizable bottom quark mass and kinematical phase space effects, and may overestimate the inclusive cross section. Very recently, it is shown in Ref. [13] that the bottom parton approach is still valid if we choose the factorization scale below the average final state mass: $\mu_f \sim C m_{\rm av} \equiv C(m_{\tilde{t}_i} + m_{\tilde{\chi}_k^-})/2$ with $C \sim (1/4, ..., 1/3)$. Thus, in this Letter, we choose $\mu_f = m_{\rm av}/3$ when we use the bottom parton approximations.

The leading order (LO) associated production of stops and charginos proceeds through the subprocess $g(p_a)b(p_b) \to \tilde{t}_i(p_1)\tilde{\chi}_k^-(p_2)$ with an s-channel and a t-channel. The LO squared matrix element in $n = 4 - 2\epsilon$ dimensions, which has been summed the colors and spins of the outgoing particles, and averaged over the colors and spins of the incoming ones, is given by

$$\overline{|M_{ik}^B|}^2 = \frac{g_s^2}{12(1-\epsilon)}(|l_{ik}^{\tilde{t}}|^2 + |k_{ik}^{\tilde{t}}|^2)(-\frac{t_2 + (1-\epsilon)u_2}{s} + \frac{ss_\Delta - u_1(u_2+2t_2)}{st_1} + \frac{2t_2 m_{\tilde{t}_i}^2}{t_1^2}), \quad (1)$$

with

$$\begin{aligned} &s = (p_a + p_b)^2, \quad s_\Delta = s - m_{\tilde{t}_i}^2 - m_{\tilde{\chi}_k^-}^2, \\ &t = (p_a - p_1)^2, \quad t_1 = t - m_{\tilde{t}_i}^2, \quad t_2 = t - m_{\tilde{\chi}_k^-}^2, \\ &u = (p_a - p_2)^2, \quad u_1 = u - m_{\tilde{t}_i}^2, \quad u_2 = u - m_{\tilde{\chi}_k^-}^2. \end{aligned} \quad (2)$$

In Eq. (1), $l_{ik}^{\tilde{t}}$ and $k_{ik}^{\tilde{t}}$ are the left- and right-handed coupling constants of the vertex b–$\tilde{t}_i$–$\tilde{\chi}_k^-$, respectively, and are defined as follows:

$$l_{ik}^{\tilde{t}} = -gR_{i1}^{\tilde{t}}V_{k1}^* + \frac{gm_t}{\sqrt{2}m_W \sin\beta}R_{i2}^{\tilde{t}}V_{k2}^*, \qquad k_{ik}^{\tilde{t}} = \frac{gm_b}{\sqrt{2}m_W \cos\beta}R_{i1}^{\tilde{t}}U_{k2}. \quad (3)$$

Here the angle β is defined by $\tan\beta \equiv v_2/v_1$, the ratio of the vacuum expectation values of the two Higgs doublets. Matrices U/V and $R^{\tilde{t}}$ are the chargino and top squark transformation matrices from interaction to mass eigenstates [14], respectively.

The NLO corrections to the cross sections can be separated into the virtual corrections arising from loop diagrams of colored particles and the real corrections arising from the radiations of a real gluon or a massless (anti)quark. The virtual corrections consist of the interference of the LO amplitude M_{ik}^B with the one-loop amplitudes M_{ik}^V containing the counterterms and the self-energy, vertex and box diagrams. We carried out the calculation in t'Hooft-Feynman gauge and used the dimensional regularization in $n = 4-2\epsilon$ dimensions to regularize the ultraviolet (UV), soft infrared and collinear divergences in the virtual loop corrections. However, this method violates the supersymmetry. In order to restore the supersymmetry the simplest procedure is through finite shifts in the quark-squark-chargino couplings [15]. As for the Dirac matrix γ_5, we deal with it using the "naive" scheme, in which the γ_5-matrix anticommutes with the other γ_μ-matrices. This is a legitimate procedure at the one-loop level for anomaly-free theories [16]. The QCD coupling constant g_s is renormalized in the modified minimal subtraction ($\overline{MS}$) scheme except that the divergences associated

with the top-quark and colored SUSY particle loops are subtracted at zero momentum [4, 17]. The other renormalization constants are fixed by the on-mass-shell renormalization scheme [18], and the renormalization constant of the stop mixing angle is fixed as shown in Ref. [19]. After renormalization, M^V_{ik} is UV-finite, but it still contains the infrared (IR) divergences which can be expressed as

$$M^V_{ik}|_{IR} = \frac{\alpha_s}{2\pi}\Gamma(1+\epsilon)(\frac{4\pi\mu_r^2}{s})^\epsilon(\frac{A_2^V}{\epsilon^2}+\frac{A_1^V}{\epsilon})M^B_{ik}, \tag{4}$$

where

$$A_2^V = -\frac{13}{3}, \qquad A_1^V = -\frac{43}{6}-\frac{4}{3}\ln\frac{s}{m^2_{\tilde{t}_i}}+3\ln\frac{-t_1}{m^2_{\tilde{t}_i}}-\frac{1}{3}\ln\frac{-u_1}{m^2_{\tilde{t}_i}}. \tag{5}$$

Here the infrared divergences include the soft infrared divergences and the collinear infrared divergences.

The real corrections arising from the real gluon emission $gb \to \tilde{t}_i\tilde{\chi}_k^- g$ will produce infrared singularities, which can be either soft or collinear. These singularities can be conveniently isolated by the two cutoff phase space slicing method [20], in which two cutoffs δ_s and δ_c are introduced, and the partonic cross section of the real gluon emission can be written as

$$\hat{\sigma}^R_{ik} = \hat{\sigma}^S_{ik} + \hat{\sigma}^{HC}_{ik} + \hat{\sigma}^{\overline{HC}}_{ik}. \tag{6}$$

Here the hard non-collinear part $\hat{\sigma}^{\overline{HC}}_{ik}$ is finite and can be numerically computed using standard Monte-Carlo integration techniques [21]. The soft part $\hat{\sigma}^S_{ik}$ contains all the soft infrared divergences, and is given by

$$\hat{\sigma}^S_{ik} = \hat{\sigma}^B[\frac{\alpha_s}{2\pi}\frac{\Gamma(1-\epsilon)}{\Gamma(1-2\epsilon)}(\frac{4\pi\mu_r^2}{s})^\epsilon](\frac{A_2^s}{\epsilon^2}+\frac{A_1^s}{\epsilon}+A_0^s) \tag{7}$$

with

$$\begin{aligned}
A_2^s &= \frac{13}{3}, \qquad A_1^s = -2A_2^s\ln\delta_s + \frac{4}{3}+\frac{1}{3}\ln\frac{-u_1}{m^2_{\tilde{t}_i}}-3\ln\frac{-t_1}{m^2_{\tilde{t}_i}}+\frac{4}{3}\ln\frac{s}{m^2_{\tilde{t}_i}},\\
A_0^s &= 2A_2^s\ln^2\delta_s - 2A_1^s\ln\delta_s + (\frac{4}{3}\frac{\gamma}{\beta}-\frac{1}{4})\ln\frac{\gamma+\beta}{\gamma-\beta}+\frac{1}{2}\ln^2\frac{s(\beta-\gamma)}{t_1}+\mathrm{Li}_2[1+\frac{t_1}{s(\gamma-\beta)}]\\
&\quad -\mathrm{Li}_2[1+\frac{s(\gamma+\beta)}{t_1}]+\frac{1}{6}\{\ln^2\frac{s(\beta-\gamma)}{u_1}-\frac{1}{2}\ln^2\frac{\gamma+\beta}{\gamma-\beta}+2\mathrm{Li}_2[\frac{t_1+s(\beta+\gamma)}{s(\beta-\gamma)}]\\
&\quad -2\mathrm{Li}_2[\frac{t_1+s(\beta-\gamma)}{-u_1}]\},
\end{aligned} \tag{8}$$

where $\gamma = (s+m^2_{\tilde{t}_i}-m^2_{\tilde{\chi}_k^-})/(2s)$ and $\beta = \sqrt{\gamma^2 - m^2_{\tilde{t}_i}/s}$. The hard collinear part $\hat{\sigma}^{HC}_{ik}$ contains the collinear divergences, and is given by [20]

$$d\sigma^{HC}_{ik} = d\hat{\sigma}^B_{ik}[\frac{\alpha_s}{2\pi}\frac{\Gamma(1-\epsilon)}{\Gamma(1-2\epsilon)}(\frac{4\pi\mu_r^2}{s})^\epsilon](-\frac{1}{\epsilon})\delta_c^{-\epsilon}[P_{bb}(z,\epsilon)G_{b/p}(x_1/z)G_{g/p}(x_2) + P_{gg}(z,\epsilon)G_{g/p}(x_1/z)G_{b/p}(x_2) + (x_1 \leftrightarrow x_2)]\frac{dz}{z}(\frac{1-z}{z})^{-\epsilon}dx_1dx_2, \quad (9)$$

where $G_{b(g)/p}(x)$ is the bare parton distribution function (PDF), and the unregulated splitting functions $P_{ij}(z,\epsilon)$ can be related to the Altarelli-Parisi splitting kernels [22] as $P_{ij}(z,\epsilon) = P_{ij}(z) + \epsilon P'_{ij}(z)$, explicitly

$$P_{qq}(z) = C_F\frac{1+z^2}{1-z}, \qquad P'_{qq}(z) = -C_F(1-z),$$
$$P_{gg}(z) = 2N[\frac{z}{1-z} + \frac{1-z}{z} + z(1-z)], \qquad P'_{gg}(z) = 0 \quad (10)$$

with $C_F = 4/3$ and $N = 3$.

In addition to the real gluon emission, other real emission corrections to the inclusive cross section for $pp \to \tilde{t}_i\tilde{\chi}_k^-$ at NLO involve the processes with an additional massless (anti)quark in the final states ($q = u, d, s, c$):

$$g + g \to \tilde{t}_i + \tilde{\chi}_k^- + \bar{b}, \quad (11)$$
$$q/\bar{q} + b \to \tilde{t}_i + \tilde{\chi}_k^- + q/\bar{q}, \quad (12)$$
$$b/\bar{b} + b \to \tilde{t}_i + \tilde{\chi}_k^- + b/\bar{b}, \quad (13)$$
$$q + \bar{q} \to \tilde{t}_i + \tilde{\chi}_k^- + \bar{b}. \quad (14)$$

Since the contributions from the processes (11)-(13) contain the initial state collinear singularities, we also need to use the two cutoff phase space slicing method [20]. However, we only split the phase space into two regions, because there are no soft divergences here. Thus, according to the approach shown in Ref. [20], the cross sections for the processes with an additional massless quark in the final states can be expressed as ($q = u, d, s, c, b$)

$$d\sigma^{add}_{ik} = \sum_{(\alpha,\beta)}\hat{\sigma}^{\overline{C}}_{ik}(\alpha\beta \to \tilde{t}_i\tilde{\chi}_k^- + X)[G_{\alpha/p}(x_1)G_{\beta/p}(x_2) + (x_1 \leftrightarrow x_2)]dx_1dx_2 + d\hat{\sigma}^B_{ik}[\frac{\alpha_s}{2\pi}\frac{\Gamma(1-\epsilon)}{\Gamma(1-2\epsilon)}(\frac{4\pi\mu_r^2}{s})^\epsilon](-\frac{1}{\epsilon})\delta_c^{-\epsilon}[P_{bg}(z,\epsilon)G_{g/p}(x_1/z)G_{g/p}(x_2) + \sum_{\alpha=q,\bar{q}}P_{g\alpha}(z,\epsilon)G_{\alpha/p}(x_1/z)G_{b/p}(x_2) + (x_1 \leftrightarrow x_2)]\frac{dz}{z}(\frac{1-z}{z})^{-\epsilon}dx_1dx_2, \quad (15)$$

where

$$P_{gq}(z) = C_F \frac{1+(1-z)^2}{z}, \qquad P'_{gq}(z) = -C_F z,$$
$$P_{qg}(z) = \frac{1}{2}[z^2+(1-z)^2], \qquad P'_{qg}(z) = -z(1-z). \tag{16}$$

The first term in Eq.(15) represents the non-collinear cross sections for the four processes. Moreover, for the subprocesses $gg/q\bar{q} \to \tilde{t}_i\bar{\tilde{t}}_i^* \to \tilde{t}_i\tilde{\chi}_k^-\bar{b}$ ($q = u, d, c, s, b$), assuming $m_{\tilde{t}_i} > m_{\tilde{\chi}_k^-}$, the stop momentum can approach the $m_{\tilde{t}_i}$ mass shell, which will lead to singularity arising from the stop propagator. Following the analysis shown in Ref. [4], this problem can easily be solved by introducing the non-zero stop widths $\Gamma_{\tilde{t}_i}$ and regularizing in this way the higher-order amplitudes. However, these on-shell stop contributions are already accounted for by the LO stop pair production with a subsequent decay into a chargino and a bottom quark, and thus should not be considered as a genuine higher order correction to the associated production of top squarks and charginos. Therefore, to avoid double counting, these pole contributions will be subtracted in our numerical calculations below in the same way as shown in Appendix B of Ref. [4].

After adding the renormalized virtual and real corrections, the partonic cross sections still contain the collinear divergences, which can be absorbed into the redefinition of the PDF at NLO, in general called mass factorization [23]. This procedure in practice means that first we convolute the partonic cross section with the bare PDF $G_{\alpha/p}(x)$, and then use the renormalized PDF $G_{\alpha/p}(x,\mu_f)$ to replace $G_{\alpha/p}(x)$. In the $\overline{\rm MS}$ convention, the scale dependent PDF $G_{\alpha/p}(x,\mu_f)$ is given by [20]

$$G_{\alpha/p}(x,\mu_f) = G_{\alpha/p}(x) + \sum_\beta (-\frac{1}{\epsilon})[\frac{\alpha_s}{2\pi}\frac{\Gamma(1-\epsilon)}{\Gamma(1-2\epsilon)}(\frac{4\pi\mu_r^2}{\mu_f^2})^\epsilon]\int_x^1 \frac{dz}{z} P_{\alpha\beta}(z) G_{\beta/p}(x/z). \tag{17}$$

This replacement will produce a collinear singular counterterm, which is combined with the hard collinear contributions to result in, as the definition in Ref. [20], the $\mathcal{O}(\alpha_s)$ expression for the remaining collinear contribution:

$$\begin{aligned} d\sigma_{ik}^{coll} = d\hat{\sigma}_{ik}^B [\frac{\alpha_s}{2\pi}\frac{\Gamma(1-\epsilon)}{\Gamma(1-2\epsilon)}(\frac{4\pi\mu_r^2}{s})^\epsilon]\{&\tilde{G}_{g/p}(x_1,\mu_f)G_{b/p}(x_2,\mu_f) + G_{g/p}(x_1,\mu_f)\tilde{G}_{b/p}(x_2,\mu_f) \\ &+ \sum_{\alpha=b,g}[\frac{A_1^{sc}(\alpha\to\alpha g)}{\epsilon} + A_0^{sc}(\alpha\to\alpha g)]G_{g/p}(x_1,\mu_f)G_{b/p}(x_2,\mu_f) \\ &+ (x_1 \leftrightarrow x_2)\}dx_1 dx_2 \end{aligned} \tag{18}$$

where

$$A_1^{sc}(q\to qg) = C_F(2\ln\delta_s + 3/2), \tag{19}$$

$$A_1^{sc}(g \to gg) = 2N \ln \delta_s + (11N - 2n_f)/6, \tag{20}$$

$$A_0^{sc} = A_1^{sc} \ln(\frac{s}{\mu_f^2}), \tag{21}$$

$$\tilde{G}_{\alpha/p}(x, \mu_f) = \sum_\beta \int_x^{1-\delta_s\delta_{\alpha\beta}} \frac{dy}{y} G_{\beta/p}(x/y, \mu_f) \tilde{P}_{\alpha\beta}(y) \tag{22}$$

with

$$\tilde{P}_{\alpha\beta}(y) = P_{\alpha\beta} \ln(\delta_c \frac{1-y}{y} \frac{s}{\mu_f^2}) - P'_{\alpha\beta}(y). \tag{23}$$

Finally, the NLO total cross section for $pp \to \tilde{t}_i \tilde{\chi}_k^-$ in the $\overline{MS}$ factorization scheme is

$$\begin{aligned}\sigma_{ik}^{NLO} = &\int \{dx_1 dx_2 [G_{b/p}(x_1, \mu_f) G_{g/p}(x_2, \mu_f) + x_1 \leftrightarrow x_2](\hat{\sigma}_{ik}^B + \hat{\sigma}_{ik}^V + \hat{\sigma}_{ik}^S + \hat{\sigma}_{ik}^{\overline{HC}}) + d\sigma_{ik}^{coll}\} \\ &+ \sum_{(\alpha,\beta)} \int dx_1 dx_2 [G_{\alpha/p}(x_1, \mu_f) G_{\beta/p}(x_2, \mu_f) + (x_1 \leftrightarrow x_2)] \hat{\sigma}_{ik}^{\overline{C}}(\alpha\beta \to \tilde{t}_i \tilde{\chi}_k^- + X).\end{aligned} \tag{24}$$

Note that the above expression contains no singularities since $A_2^V + A_2^s = 0$ and $A_1^V + A_1^s + A_1^{sc}(b \to bg) + A_1^{sc}(g \to gg) = 0$. The explicit expressions of $\hat{\sigma}_{ik}^V$, $\hat{\sigma}_{ik}^{\overline{HC}}$ and $\hat{\sigma}_{ik}^{\overline{C}}$ have been given in Ref. [24].

We now present some typical numerical results for total cross sections for the associated production of top squarks and charginos at the LHC. In our numerical calculations the Standard Model (SM) parameters were taken to be $\alpha_{ew}(m_W) = 1/128$, $m_W = 80.419$ GeV, $m_Z = 91.1882$ GeV, and $m_t = 174.3$ GeV [25]. We use the two-loop evolution of $\alpha_s(\mu)$ [26] ($\alpha_s(M_Z) = 0.118$), and CTEQ6M (CTEQ6L) PDFs [27] throughout the calculations of the NLO (LO) cross sections. Moreover, in order to improve the perturbative calculations, we take the running mass $m_b(Q)$ evaluated by the NLO formula [28] with $m_b(m_b) = 4.25$ GeV [29], and make the following replacement in the tree-level couplings [28]:

$$m_b(Q) \quad \to \quad \frac{m_b(Q)}{1 + \Delta m_b}, \tag{25}$$

with

$$\begin{aligned}\Delta m_b = &\frac{2\alpha_s}{3\pi} m_{\tilde{g}} \mu \tan\beta I(m_{\tilde{b}_1}, m_{\tilde{b}_2}, m_{\tilde{g}}) + \frac{g^2 m_t^2}{16\pi^2 m_W^2 \sin 2\beta} \mu A_t I(m_{\tilde{t}_1}, m_{\tilde{t}_2}, \mu) \\ &- \frac{g^2}{16\pi^2} \mu M_2 \tan\beta \sum_{i=1}^{2} [(R_{i1}^{\tilde{t}})^2 I(m_{\tilde{t}_i}, M_2, \mu) + \frac{1}{2}(R_{i1}^{\tilde{b}})^2 I(m_{\tilde{b}_i}, M_2, \mu)]\end{aligned} \tag{26}$$

where A_t is the soft SUSY-breaking parameter, μ is the Higgs mixing parameter in the superpotential, and

$$I(a, b, c) = \frac{1}{(a^2 - b^2)(b^2 - c^2)(a^2 - c^2)} (a^2 b^2 \log\frac{a^2}{b^2} + b^2 c^2 \log\frac{b^2}{c^2} + c^2 a^2 \log\frac{c^2}{a^2}). \tag{27}$$

In order to avoid double counting, it is necessary to subtract these (SUSY-)QCD corrections from the renormalization constant δm_b in the following numerical calculations. In the calculations of the stop decay width $\Gamma_{\tilde{t}_i}$, the two-loop leading-log relations [30] of the neutral Higgs boson masses and mixing angles in the MSSM were used, and the CP-odd Higgs boson mass m_{A^0} was fixed to 200 GeV. For the charged Higgs boson mass the tree-level formula was used. Other MSSM parameters are determined as follows: (i) For the parameters M_1, M_2 and μ in the chargino and neutralino matrices, we take M_2 and μ as the input parameters, and assuming gaugino mass unification we take $M_1 = (5/3)\tan^2\theta_W M_2$ and $m_{\tilde{g}} = (\alpha_s(m_{\tilde{g}})/\alpha_2)M_2$ [31]. (ii) For the parameters in squark mass matrices, we assume $M_{\tilde{Q}} = M_{\tilde{U}} = M_{\tilde{D}}$ and $A_t = A_b = 300$ GeV to simplify the calculations. Actually, the numerical results are not very sensitive to $A_{t(b)}$. Moreover, except in Fig.2, we always choose the renormalization scale $\mu_r = m_{\rm av}$, and the factorization scale μ_f is fixed to $m_{\rm av}/3$.

Fig.1 shows the $m_{\tilde{t}_1}$ dependence of the LO and NLO predictions for $pp \to \tilde{t}_i\tilde{\chi}_k^-$, assuming $\mu = -200$ GeV, $M_2 = 300$ GeV and $\tan\beta = 30$, which means that two chargino masses are about 182 GeV and 331 GeV, respectively, and $m_{\tilde{t}_2}$ increases from 342 GeV to 683 GeV for $m_{\tilde{t}_1}$ in the range 100–600 GeV. One finds that the total cross section for the $\tilde{t}_2\tilde{\chi}_2^-$ channel is always smallest and less than 3 fb, but the total cross sections for other channels are large and range between 10 fb and several hundred fb for most values of $m_{\tilde{t}_1}$. Especially for the $\tilde{t}_1\tilde{\chi}_1^-$ channel, the total cross section can reach 1 pb for small values of $m_{\tilde{t}_1}$ (100 GeV $< m_{\tilde{t}_1} <$ 160 GeV), which is almost the same as ones of top quark and charged Higgs boson associated production at the LHC. However, when $m_{\tilde{t}_1}$ gets larger and close to $m_{\tilde{t}_2}$, the total cross section for the $\tilde{t}_2\tilde{\chi}_1^-$ channel is the largest. Moreover, Fig.1 also shows that the NLO QCD corrections enhance the LO results significantly, which are in general a few ten percent. The associated production of $\tilde{t}_1$ and $\tilde{\chi}_1^-$ is the most important since the total cross sections are the largest for $m_{\tilde{t}_1} < 400$ GeV. Thus we mainly discuss this channel below.

In Fig.2 we show the dependence of the total cross sections for the $\tilde{t}_1\tilde{\chi}_1^-$ production on the renormalization/factorization scale, assuming $\mu = -200$ GeV, $M_2 = 300$ GeV, $\tan\beta = 30$, $m_{\tilde{t}_1} = 250$ GeV, and $\mu_r = \mu_f$. One finds that the NLO QCD corrections reduce the dependence significantly. The cross sections vary by $\pm 15\%$ at LO but only by $\pm 4\%$ at NLO in the region $0.5 < \mu_f/m_{\rm av} < 2.0$. Thus the reliability of the NLO predictions has a substantial improvement.

The cross sections of the $\tilde{t}_1\tilde{\chi}_1^-$ production as a function of $\tan\beta$ are displayed for $m_{\tilde{t}_1} =$

200, 300 and 400 GeV in Fig.3, assuming $\mu = -200$ GeV and $M_2 = 300$ GeV. From Fig.3, one can see that the cross sections become large when $\tan\beta$ gets high or low, which is due to the fact that for the coupling $b-\tilde{t}_1-\tilde{\chi}_1^-$ at low $\tan\beta$ the top quark contribution is enhanced while at high $\tan\beta$ the bottom quark contribution becomes large. Fig.3 also shows that the NLO QCD corrections enhance the LO total cross sections, and for $m_{\tilde{t}_1} = 200$ and 300 GeV, the enhancement is more significant for the medium values of $\tan\beta$ than for the high and low ones.

In conclusion, we have calculated the NLO inclusive total cross sections for the associated production processes $pp \to \tilde{t}_i\tilde{\chi}_k^-$ in the MSSM at the LHC. Our calculations show that the total cross sections for the $\tilde{t}_1\tilde{\chi}_1^-$ production for the lighter top squark masses in the region 100 GeV $< m_{\tilde{t}_1} <$ 160 GeV can reach 1 pb in the favorable parameter space allowed by the current precise experiments, and besides the above case the total cross sections generally vary from 10 fb to several hundred fb except both $m_{\tilde{t}_1} > 500$ GeV and the $\tilde{t}_2\tilde{\chi}_2^-$ production channel, which means that the LHC may produce abundant events of these processes, and it is very possible to discover these SUSY particles through the above processes in the future experiments, if the supersymmetry exists. Moreover, we find that the NLO QCD corrections in general enhance the LO total cross sections significantly, and vastly reduce the dependence of the total cross sections on the renormalization/factorization scale, which leads to increased confidence in predictions based on these results.

Acknowledgments

We would like to thank T. Plehn and C.-P. Yuan for useful discussions and valuable suggestions. This work was supported in part by the National Natural Science Foundation of China.

---

[1] F. Gianotti, M.L. Mangano, T. Virdee, hep-ph/0204087.

[2] H.P. Nilles, Phys. Rep. 110 (1984) 1; H.E. Haber and G.L. Kane, Phys. Rep. 117 (1985) 75; A.B. Lahanas, D.V. Nanopoulos, Phys. Rep. 145 (1987) 1; Supersymmetry, Vols. 1 and 2, ed. S. Ferrara (North Holland/World Scientific, Singapore, 1987). For a recent review, consult S. Dawson, TASI-97 lectures, hep-ph/9712464.

[3] G.L. Kane and J.P. Leveille, Phys. Lett. B 112 (1982) 227; P.R. Harrison and C.H. Llewellyn Smith, Nucl. Phys. B 213 (1983) 223; Nucl. Phys. B 223 (1983) 542 (E); E. Reya and D.P. Roy, Phys. Rev. D 32 (1985) 645; S. Dawson, E. Eichten, C. Quigg, Phys. Rev. D 31 (1985) 1581; H. Baer and X. Tata, Phys. Lett. B 160 (1985) 159.

[4] W. Beenakker, R. Höpker, M. Spira, P.M. Zerwas, Nucl. Phys. B 492 (1997) 51.

[5] W. Beenakker, R. Höpker, M. Spira, P.M. Zerwas, Phys. Rev. Lett. 74 (1995) 2905; Z. Phys. C 69 (1995) 163.

[6] W. Beenakker, M. Krämer, T. Plehn, P.M. Zerwas, Nucl. Phys. B 515 (1998) 3.

[7] W. Beenakker, M. Klasen, M. Krämer, T. Plehn, M. Spira, P.M. Zerwas, Phys. Rev. Lett. 83 (1999) 3780.

[8] H. Baer, B.W. Harris, M.H. Reno, Phys. Rev. D 57 (1998) 5871.

[9] E.L. Berger, M. Klasen, T.M.P. Tait, Phys. Lett. B 459 (1999) 165; Phys. Rev. D 62 (2000) 095014.

[10] J.F. Gunion, H.E. Haber, F.E. Paige, W.-K. Tung, S. Willenbrock, Nucl. Phys. B 294 (1987) 621; R.M. Barnett, H.E. Haber, D.E. Soper, Nucl. Phys. B 306 (1988) 697; F.I. Olness and W.-K. Tung, Nucl. Phys. B 308 (1988) 813; V. Barger, R.J.N. Phillips, D.P. Roy, Phys. Lett. B 324 (1994) 236; C.S. Huang and S.H. Zhu, Phys. Rev. D 60 (1999) 075012; L.G. Jin, C.S. Li, R.J. Oakes, S.H. Zhu, Phys. Rev. D 62 (2000) 053008; S.H. Zhu, hep-ph/0112109.

[11] M. A. Aivazis, J. C. Collins, F. I. Olness, and W. K. Tung, Phys. Rev. D 50 (1994) 3102; J. C. Collins, Phys. Rev. D 58 (1998) 094002; M. Kramer, F. I. Olness, D. E. Soper, Phys. Rev. D 62 (2000) 096007.

[12] D. Cavalli, *et al.*, 'The Higgs working group: Summary Report', Los Houches 2001, "Physics at TeV Colliders", hep-ph/0203056; D. Rainwater, M. Spira, D. Zeppenfeld, hep-ph/0203187; M. Spira, hep-ph/0211145.

[13] T. Plehn, hep-ph/0206121; F. Maltoni, Z. Sullivan, S. Willenbrock, hep-ph/0301033.

[14] J.F. Gunion and H. Haber, Nucl. Phys. B 272 (1986) 1.

[15] W. Beenakker, R. Höpker, P.M. Zerwas, Phys. Lett. B 378 (1996) 159; W. Beenakker, R. Höpker, T. Plehn, P.M. Zerwas, Z. Phys. C 75 (1997) 349.

[16] M. Chanowitz, M. Furman, I. Hinchliffe, Nucl. Phys. B 159 (1979) 225.

[17] J. Collins, F. Wilczek, A. Zee, Phys. Rev. D 18 (1978) 242; W. J. Marciano, Phys. Rev. D 29 (1984) 580; Phys. Rev. D 31 (1984) 213 (E); P. Nason, S. Dawson, R.K. Ellis, Nucl. Phys. B

327 (1989) 49; Nucl. Phys. B 335 (1989) 260 (E).

[18] A. Sirlin, Phys. Rev. D 22 (1980) 971; W. J. Marciano and A. Sirlin, Phys. Rev. D 22 (1980) 2695; Phys. Rev. D 31 (1985) 213 (E); A. Sirlin and W.J. Marciano, Nucl. Phys. B 189 (1981) 442; K.I. Aoki et.al., Prog. Theor. Phys. Suppl. 73 (1982) 1.

[19] J. Guasch, W. Hollik, J. Solà, Phys. Lett. B 437 (1998) 88.

[20] B.W. Harris and J.F. Owens, Phys. Rev. D 65 (2002) 094032.

[21] G.P. Lepage, J. Comp. Phys. 27 (1978) 192.

[22] G. Altarelli and G. Parisi, Nucl. Phys. B 126 (1977) 298.

[23] G. Altarelli, R.K. Ellis, G. Martinelli, Nucl. Phys. B 157 (1979) 461; J.C. Collins, D.E. Soper, G. Sterman, in: Perturbative Quantum Chromodynamics, ed. A.H. Mueller (World Scientific, 1989).

[24] Li Gang Jin, Chong Sheng Li, Jian Jun Liu, hep-ph/0210362.

[25] Particle Data Group, D.E. Groom et al, Eur. Phys. J. C 15 (2000) 1.

[26] S.G. Gorishny, A.L. Kataev, S.A. Larin, L.R. Surguladze, Mod. Phys. Lett. A 5 (1990) 2703; Phys. Rev. D 43 (1991) 1633; A. Djouadi, M. Spira, P.M. Zerwas, Z. Phys. C 70 (1996) 427; A. Djouadi, J. Kalinowski, M. Spira, Comput. Phys. Commun. 108 (1998) 56; M. Spira, Fortschr. Phys. 46 (1998) 203.

[27] J. Pumplin, D.R. Stump, J. Huston, H.L. Lai, P. Nadolsky, W.K. Tung, hep-ph/0201195.

[28] M. Carena, D. Garcia, U. Nierste, C.E.M. Wagner, Nucl. Phys. B 577 (2000) 88.

[29] M. Beneke and A. Signer, Phys. Lett. B 471 (1999) 233; A.H. Hoang, Phys. Rev. D 61 (2000) 034005.

[30] M. Carena, M. Quirós, C.E.M. Wagner, Nucl. Phys. B 461 (1996) 407.

[31] K. Hidaka and A. Bartl, Phys. Lett. B 501 (2001) 78.

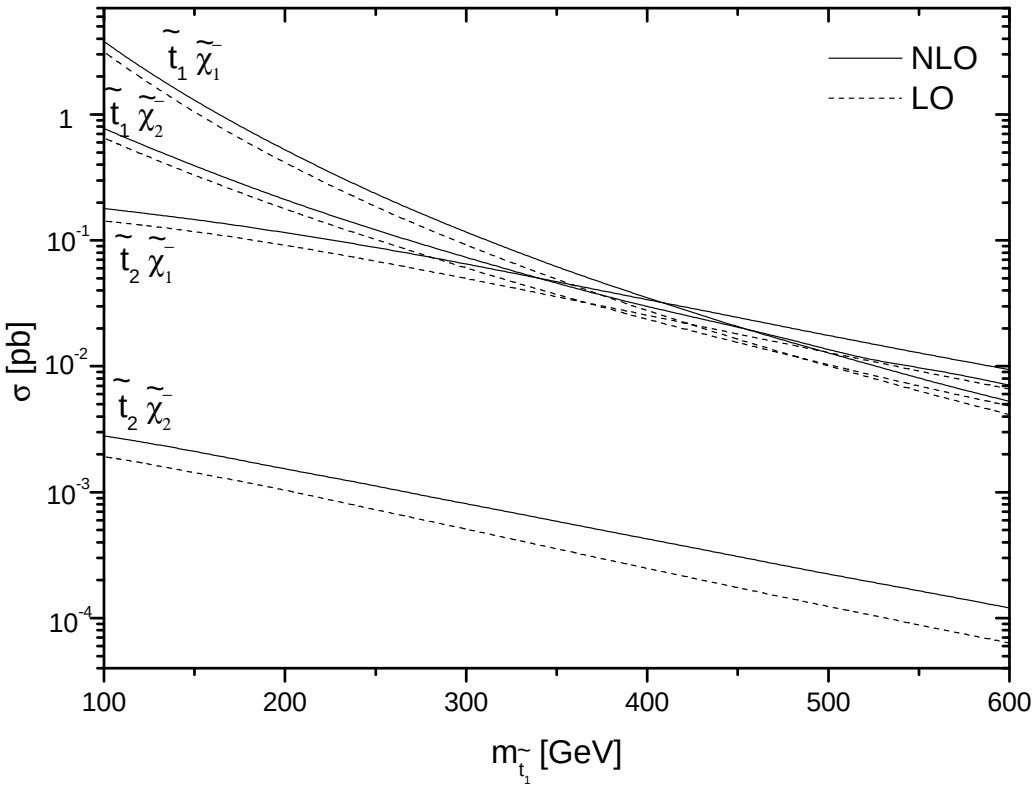

FIG. 1: Dependence of the total cross sections on $m_{\tilde{t}_1}$ for the $\tilde{t}_i\tilde{\chi}_k^-$ productions at the LHC, assuming $\mu = -200$ GeV, $M_2 = 300$ GeV and $\tan\beta = 30$.

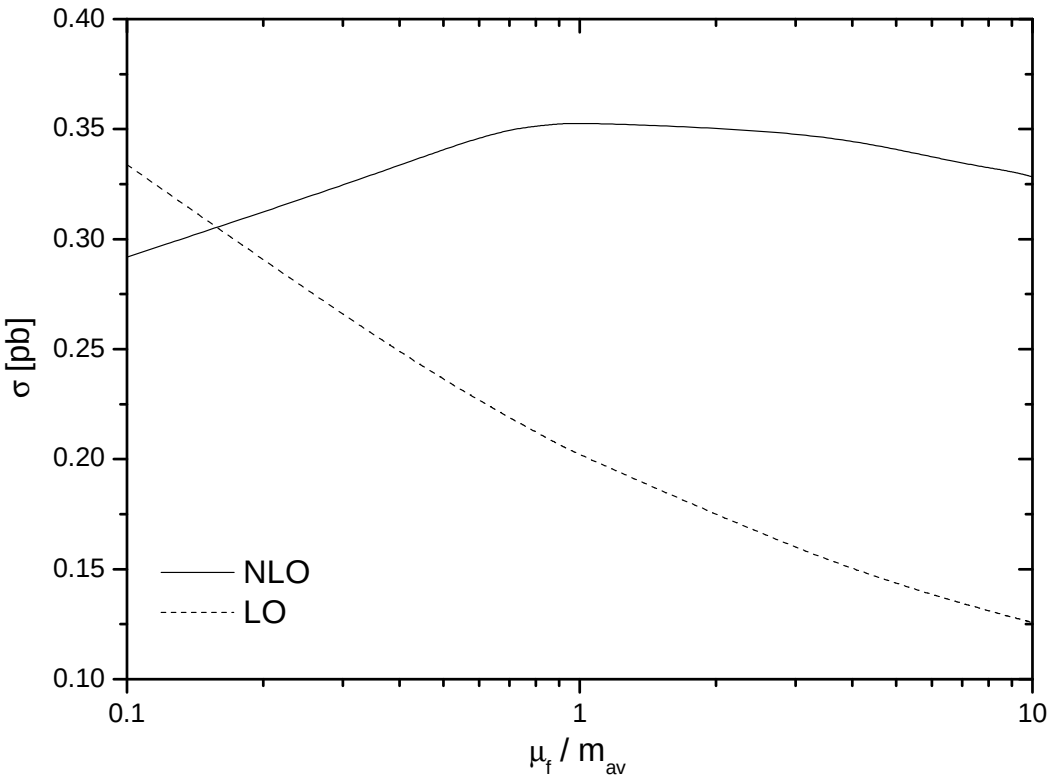

FIG. 2: Dependence of the total cross sections for the $\tilde{t}_1\tilde{\chi}_1^-$ production at the LHC on the renormalization/factorization scale, assuming $\mu = -200$ GeV, $M_2 = 300$ GeV, $\tan\beta = 30$, $m_{\tilde{t}_1} = 250$ GeV, $\mu_r = \mu_f$ and $m_{\rm av} = (m_{\tilde{t}_1} + m_{\tilde{\chi}_1^-})/2$.

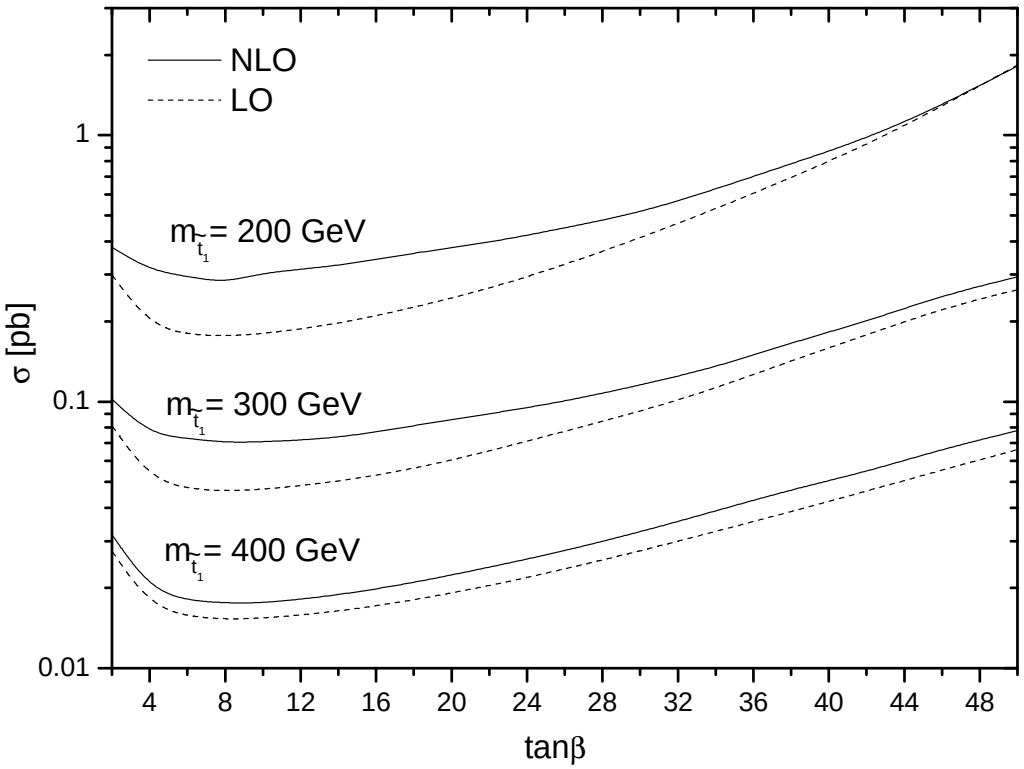

FIG. 3: Dependence of the total cross sections for the $\tilde{t}_1\tilde{\chi}_1^-$ production at the LHC on the parameter $\tan\beta$, assuming $\mu = -200$ GeV and $M_2 = 300$ GeV.